Mechanical behaviour assessment of the Ti6Al4V alloy obtained by additive manufacturing towards aeronautical industry

Daniel García Hernández
Instituto Superior Técnico
E-mail: dagarhe3@gmail.com

Abstract

Nowadays the dynamics of markets, technology advances, and companies' competition have brought changes in metal processing. Recent technical improvements of additive manufacturing (AM) have shifted the application of these processes from prototyping to the production of end-use parts either as customised or series. The extended geometric flexibility, coupled with the reduced time of production and the improved efficiency in resources utilization inherent of Selective laser melting (SLM) are the characteristics sought by aircraft industry in order to develop and progress.

This thesis aims to contribute to the study and analysis of a new strategy of production Selective Laser Melting in the manufacture of metallic components for aeronautical use. Specifically the mechanical characterization of the titanium alloy Ti6Al4V is performed. For this purpose several samples and specimens were manufactured in the SLM equipment of CDRSP (Centre for Rapid and Sustainable Product Development) and the mechanical tests were carried out at the Instituto Superior Técnico (IST).

SLM is an additive manufacturing technique through which components are built by selectively melting powder layers with a focused laser beam. With the proper setting of the SLM process, a relative density above the required value in the aircraft industry (above 99%) is achieved. Specifically in this work, relative densities of around 99.6% were achieved. However the process is characterized by short laser-powder interaction times and localized high heat input, which leads to steep thermal gradients, rapid solidification and fast cooling resulting in a specific microstructure. In order to obtain optimal mechanical properties, heat treatments are necessary due to the original martensitic microstructure. Moreover finishing mechanical process will be required, firstly due to the need of remove the parts from the platform and secondly to decrease the surface roughness.

Keywords: Additive layer manufacturing, selective laser melting (SLM), shaped metal deposition, Ti6Al4V titanium alloy.

A special thanks to CEIIA and CDRSP for the opportunity to work in this line of research.

1. INTRODUCTION

The aircraft industry is a sector which is always looking for new developments and progress because of his tendency to grow rapidly. One of the techniques that has gained prominence in the aerospace industry is the near-net-shape Additive Manufacturing (AM). This method has significant advantages such as, more geometric freedom, shortened design to product time, reduction in process steps, component mass reduction and material flexibility. Compared with traditional methods, in general, AM contributes to the aircraft manufacturers to save time and money in the manufacturing, as well as decrease the CO_2 footprint from an environment viewpoint. Moreover, due to reducing the components weight, AM provides the possibility to produce lighter aircrafts saving both of costs to the airlines and pollution emissions, as the saying goes: "every kilogram that can be shaved off the mass of an airframe saves at least $3500 in fuel costs over the aircraft's life span" [1]. This new concept has the potential to reach the manufacturing industry and therefore it is important to have good knowledge and mastery of it to get full development.

Objectives

Specimens of titanium alloy Ti6Al4V were manufactured by SLM and were tested with the following main goals:

- Become familiar and dominate the manufacturing process SLM.
- Assess whether is necessary to apply post-processing processes or not.
- Achieve high relative density.
- Analysis of the influence of SLM parameters, building orientation and heat treatment on the final product mechanical properties.
- Mechanical characterization and evaluation of parts.

An important thing to keep in mind in this method is the relative density. The attainable density after SLM is the first and perhaps the most important concern in this process [2]. The density determines the part´s

mechanical properties which in turn has direct influence on the component performance [3]. The objective is often to obtain 100% dense parts. This goal, however, is difficult to achieve since there is no mechanical pressure applied, as in moulding processes, SLM being only characterized by temperature effects, gravity and capillary forces during the process [2]. Because the aeronautical industry only accepts parts having less than 1 vol pct of porosity, one of the goals of this work will be to get a relative density greater than 99%.

2. LITERATURE REVIEW

Additive Manufacturing (AM) is defined as the manufacturing process of building objects adding material to previous build areas, layer upon layer, as opposed to subtractive manufacturing methodologies, such as traditional machining [4]. Synonyms are additive fabrication, additive techniques, additive layer manufacturing, layered manufacturing and solid freeform fabrication. It's also worth to mention that AM includes all applications of the technology, including modeling, prototyping, pattern-making, tool-making, and the production of end-use parts in volumes of one to thousands or more. It isn't just about prototyping as it were for almost two decades since layered manufacturing techniques started to be used.

Selective Laser Melting

Selective Laser Melting (SLM) is an AM method that uses high powered laser to melt metallic powders together to shape the product from a 3D CAD data. It uses the complete melting of the metal powder by a high powered ytterbium fibre laser as the mechanism of attachment of the particles for the manufacture of parts and components with a high degree of complexity and near full density [4].

Basically the SLM process begins with the deposition of a first layer of powder over the building platform. This layer acts as a base for the manufacture of the whole piece. The laser scans a predefined area, according to the cross-section 2D of each layer of the part, melting the powder completely. Next the platform descends the value of the layer thickness to deposit powder again. This procedure is repeated until the component is finished. At the end of the process, the build chamber and the component are cleaned. The excess powder is reused after filtering. The whole process is carried out under tightly controlled atmosphere by a flow of inert gas. This helps both to prevent contamination, to avoid the presence of oxygen and nitrogen, and to protect the system, especially the lens, of the debris expelled during the process [5]. Figure 1 schematically shows the production chamber, layout.

SLM offers several advantages over conventional techniques, such as reduction of production steps, lower time-to-market, a high level of flexibility, a high material use efficiency, a near net shape production without the need of expensive moulds and direct production based on a CAD model [6]. Furthermore, hard materials or materials with a high melting point can be processed by SLM. Most important, because of the layer-wise building, SLM enables the production of parts with a high geometrical complexity.

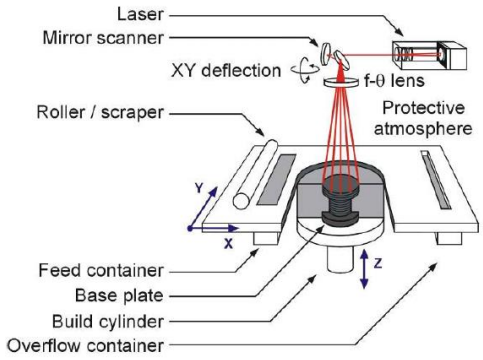

Figure 1 – Schematic view of SLM components [2].

However, the unique conditions during the SLM process give rise to some problems. Because of the short interaction times and accompanying highly localized heat input, large thermal gradients exist during the process. These lead to the build-up of thermal stresses, while the rapid solidification leads to segregation phenomena and the development of non-equilibrium phases. Moreover, non-optimal scan parameters may cause melt pool instabilities during the process, which leads to an increased porosity and a higher surface roughness [2, 6, 7]. Moreover, Attar reported [8] that the typical defects associated with SLM processes are porosity, residual powder and non-connected layers but a more substantial problem is balling phenomenon. Balling is the spheroidization of the liquid melt pool (formation of small spheres with approximately the diameter of the beam) which may lead to the formation of discontinuous scan tracks [9]. The risk of balling of the melt pool may also result in bad surface finishes [10]. Using different laser strategies may minimize thermal stresses, porosity, and shrinkage.

Key SLM Parameters

The key parameters on the final product quality are: the laser power (P), the laser beam diameter, the scanning velocity (v), the powder layer thickness (t) and the hatch space (h). All of these all illustrated in Figure 2. Other parameters to consider are the scanning strategy, the temperature of the platform and the inert atmosphere of the chamber production [7].

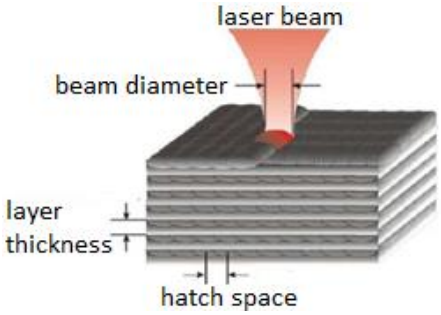

Figure 2 – SLM parameters (Image adapted from [11]).

The heating of the platform is desirable to try reduce internal stresses created during the SLM process and because fusion of powders, although it favours the hinders the extraction of heat and the consequent solidification of the layer, which may result in a porosity increase of the final component [12].

The energy density is a key factor in SLM which includes the four important parameters mentioned above, as shown in equation (*1*). Energy density needs to reach a value which ensures the melting of the powder.

$$E_{density} = \frac{P\ [W]}{v[\frac{mm}{s}] \cdot h[mm] \cdot t[mm]} \quad \left[\frac{J}{mm^3}\right] \quad (1)$$

Campanelli et al. [13] expound that too high values of energy per volume lead to an excessive melting of the layers with a substantial shrinkage and consequent balling phenomenon, which occurs when the molten material does not wet the underlying substrate due to its surface tension, which tends to spheroidise the liquid. Which means that not always that the energy density increases the relative density and the print quality is improved, but there is a limit beyond which the results worsen. On the other hand, too low values of energy density are not suitable to ensure adhesion between consecutive layers, because the penetration depth is not adequate [14].

The optimum hatch spacing is closely linked to the value of the diameter of the melt pool (diameter of the laser). Varying the hatch spacing a greater or smaller overlap is achieved and thus a more compact and hence less porous sample is obtained. It has been shown that there is an overlap value at which the porosity is minimum and increases for both sides, in other words there is a hatch space at which the relative density is maximum [5, 15].

The laser scanning strategy is the way that the laser is programmed to move its beam focus over the powder bed. A study of the influence of scanning strategy on the relative density for parts produced from Ti6Al4V powder compares three types of scanning pattern (uni-directional, zigzag and alternating strategy in which the scan line are rotated 90º in each new layer, as seen in Figure 3), showed that the zigzag alternating strategy provides the highest density [2].

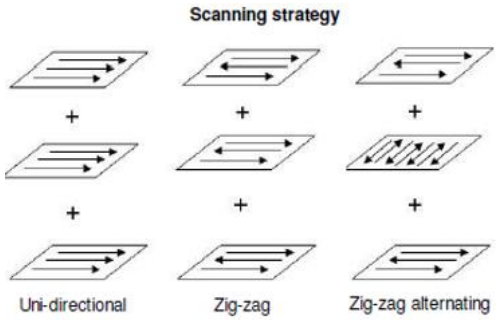

Figure 3 –schematic of applied scanning strategy [2].

In order to characterize the SLM method all the parameters that influence in the process should be studied. Process key parameters are laser power, scan velocity, layer thickness, hatch spacing, energy density, scanning strategy, etc. are optimized for the highest relative density possible (in the aircraft industry above 99%). Moreover, it is also important to study other factors such as building orientation (0 °, 45º and 0º), the post-treatments, the inert atmosphere and the powder properties (size, distribution of particle size, shape and structure). However these are not the only parameters that affect in the process, according to Rehme [16], there are 157 different factors that influence the quality of the parts obtained by SLM, including the experience of the operator.

3. MATERIALS AND METHODS

The SLM equipment used was a SLM125HL system from SLM Solutions GmbH. This machine is equipped with a YLR-Faser-Laser with a maximum power of 100 W, a 125x125x125 mm build chamber and an diameter of laser variable between 70 – 130 µm. Ti6Al4V powder (provided by SLM Solutions GmbH) with a particle size comprised between 20 and 63 µm was used.

The main process parameters such as the laser power P, the scanning speed v, the hatch space h and the layer thickness t were previously optimized to obtain the lowest porosity. For this purpose three sets of sixteen samples (in total 48 cubes) of 5x5x10 mm size were produced. A second batch of 36 cubes (three series of twelve different combinations) of 10x10x10 mm size were fabricated to determine the optimized SLM parameters.

After obtaining the optimized parameters the specimens for the mechanical characterization were fabricated. Sixteen tensile specimens (eight parallel to the build direction, TD, and eight perpendicular to the build direction, LD) and eight impact specimens (four TD and four LD) were manufactured according to ASTM Standards E 8M-01 and E 23-02a, respectively.

Post Processing

After manufacturing of the specimens was necessary to make a post processing which involved remove the specimens of the platform, final machining and heat treatment.

Before the first layers of the SLM process are built some supports are created in order to get detach the piece from the platform after the production. Besides the area of the supports, which has a worse surface quality, the general surface finish is slightly rough. The surfaces of the area to be tested should be well polished in order to remove surface defects prior to mechanical testing. The specimens were fabricated with an over thickness of 0.2 mm and were milled

Heat Treatment

From an extensive bibliographic research, it is possible to conclude that the optimal heat treatment for this work is a treatment below the β transus (± 995 °C) for 2 hours around 900 °C under vacuum atmosphere and furnace cooling. With this treatment, it is expected that the required mechanical properties will be obtained due to an optimal equilibrium condition for the formation of the α and β phases.

The influence of the temperature, residence time and cooling rate were investigated by Vrancken et al. in [6]. Based on their findings, in this research, the SLM specimens were heat-treated at 900ºC for 2 hours followed by furnace cooling in order to achieve the desired mechanical properties for aviation applications.

The treatment was carried out with a heating rate of approximately 10°C/min from room temperature until

900°C (90 minutes), a residence time of 2 hours and lastly the furnace cooling with a rate of 10-15 °C/min until room temperature (90 minutes). The length of the whole process was around 5 hours.

Densification

The densities were measured by Archimedes method with a Mettler AG204 balance and his specific density measurement device, Figure 4.

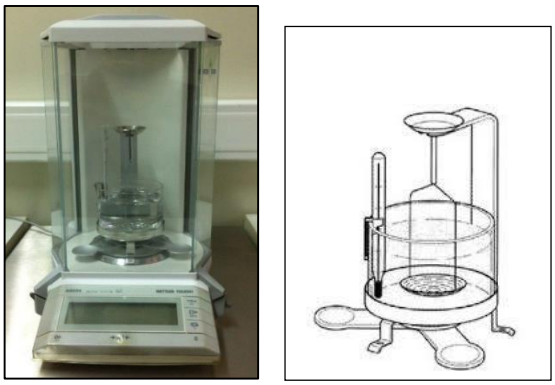

Figure 4 - Mettler AG 204 balance with the specific density measurement device.

The determination of the density ρ_p of the part under consideration was carried out according to equation (2):

$$\rho_p = \frac{m_a}{m_a - m_{fl}} \cdot \rho_{fl} \qquad (2)$$

where ρ_{fl} is the density of the fluid (deionised water), which is temperature dependent, m_a is the mass of the part in air and m_{fl} is the mass of the part in the fluid [17].

Microstructural Characterization

To observe the microstructures, the samples were mechanically ground using SiC papers up to grid 1200 and then polished using diamond paste up to 0.05 µm. To reveal the microstructure, an etchant containing 100 ml distilled H2O, 6 ml HNO3 and 3 ml HF (known as Kroll´s microetchant) was used [18]. The microstructural study was carried out on a Nikon optical microscope equipped with a digital camera system Olympus DP-10.

Hardness

Macro hardness Vickers was measured on a Mitutoyo hardness testing machine using a load of 10 kg. Both untreated and heat treated samples were evaluated in different locations using an indentation time of 30 s [15]. Samples were evaluated from one edge to the other with a 0.05 mm spacing each one in both horizontal and transversal direction to check if there are any trends.

Tensile Strength

Tensile tests are an essential tool to characterize the mechanical behaviour of materials. The specimens were produced in accordance with ASTM E 8M -01 (2012) standard. It is noteworthy that after manufacturing of the specimens by SLM they had small dimensional variations in relation to the expected standard.

Tensile tests were carried out using an Instron 3669 machine, according to the ASTM E 8M standard. To measure the elongation of the specimens an extensometer was used. Elastic modulus (E), yield stress at 0.2 per cent of elongation (σy), ultimate tensile strength (UTS) and percent elongation at fracture were determined from stress-strain curves.

The sixteen specimens were distributed as follows: 4 heat treated and LD, 4 heat treated and TD, 4 as-built and LD and 4 as-built and TD.

It was this way to study the influence on the mechanical properties of both heat treatment and manufacturing orientation. After the destructive testing, the morphological analysis of the fracture surfaces was performed.

Fractographic Analysis

A preliminary analysis of the fracture surfaces of the tensile specimens was performed using the USB Microscope VEHO® discovery VMS-004 Deluxe.

For a more detailed analysis of the defects found in the fracture surfaces a Hitachi S2400 Scanning Electron Microscope (SEM) was used. For this purpose the fracture surfaces of tensile specimens were cut and cleaned in an ultrasonic bath (acetone) before being analysed by electron microscopy.

Toughness of SLM Parts

The Charpy impact test was used to determine material toughness by hitting a test specimen with a pendulum impact tester up to 50J. A V-shaped notch was used as the impact specimen in order to control the fracture process by concentrating stress in the area of minimum cross-section. In this experimental study, Charpy tests were performed according to ASTM E23 standard. The final size was 55x10x7.5 mm despite the fact that the standard specifies 55x10x10 mm because the over thickness of the specimens was insufficient to machining. The notch used was as defined in the standard.

In this study only the influence of the orientation on the toughness was analysed, using heat treated. Four LD specimens and four TD specimens were tested.

4. RESULTS AND DISCUSSION

This research was aimed at obtaining an insight into the influence of the laser power, the scanning velocity, the hatch spacing and the energy density on the relative of the resulting samples. The aim was to find a set of parameters that would minimize the samples porosity. Secondly mechanical tests were performed to assess the influence of heat treatment and build direction on the mechanical properties of the material.

Manufacturing parameters and densification

The parameters of the first density batch were selected based both on the possibilities of the machine and data in the literature. It is found that even the highest value achieved (98.12% with P = 100 W, h = 0.08 mm and v = 500 m/s) is less than the target value (>99%). For this reason it was decided to analyse the influence and the tendency of relative density obtained according to the

parameters used and manufacture new samples with new parameters in order to attain the target value.

The trends of the sample density with respect to the energy density and hatch spacing are shown in Figure 5. In Figure 5 (a) the expected trend of increasing relative density with the energy density increase is not observed. In Figure 5 (b) an increasing trend of the density with the hatch space is detected.

In this research, the energy density – defined as the average applied energy per volume of material during the scanning of one layer – depends on laser power (P), scanning velocity (v), hatch spacing (h) and layer thickness (t), according to eq. (1); where the layer thickness is 30 µm.

Hence, it is not surprising that a direct relationship could be depicted when plotting relative density as a function of E (Figure 5 (a)). The hatch spacing, however, influences the overlap between two neighbouring scan vectors thereby affecting the melt pool width.

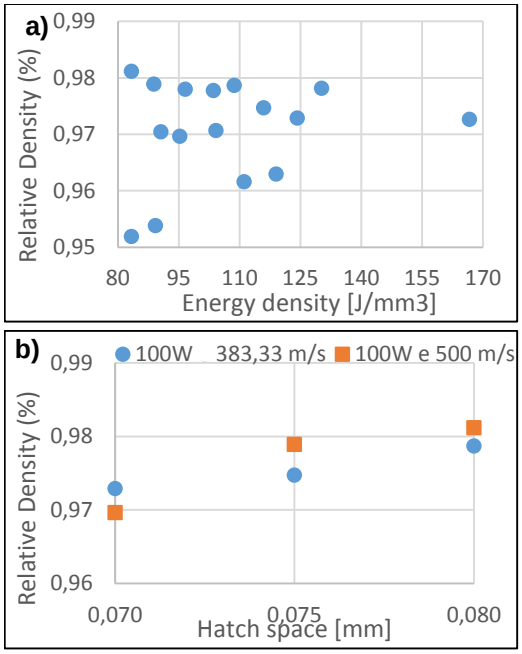

Figure 5 – a) Influence of energy density and b) hatch space on the relative density in the batch 1 results.

For a given power (100 W), it appears that above a given threshold (70 µm), the relative density seems to increase with increasing hatch spacing as shown in Figure 5 (b). Based on the observations, a new set of parameters was selected, namely hatching spacings (80, 93, 107 and 120 µm) and scanning velocities (300, 500 and 700 mm/s) were increased whereas the power was kept constant at 100 W (see Table 1).

From Table 1 it can be observed that 300 mm/s is the velocity at which higher values are obtained. This trend is in accordance with the findings in Parameters, Section 2, where it is explained that with lower speed a higher density is achieved, due to an increased energy density, recalling that there is an energy density value beyond which the relative density starts to decrease.

For Batch 2, an apparent increase in relative density is observed for energy density values higher than 60

Table 1 – Relative density results for samples from Batch 2.

	h [mm]	*v [mm/s]*	$E_{density}$ *[J/mm^3]*	*Density [%]*
1	0,080	300	139	99,06%
2	0,080	500	83	98,80%
3	0,080	700	60	97,88%
4	0,093	300	119	98,86%
5	0,093	500	71	99,03%
6	0,093	700	51	98,05%
7	0,107	300	104	98,81%
8	0,107	500	62	98,71%
9	0,107	700	45	97,53%
10	0,120	300	93	98,60%
11	0,120	500	56	98,71%
12	0,120	700	40	97,01%

J/mm3 (see Figure 7 (a)). This suggest that lower scanning velocities favour densification, as it would be expected from eq. (1). Indeed, it not surprising that the higher relative density values were obtained for the higher energy density value (Table 1).

On the other hand, under the conditions investigated, increasing hatch space above 0.08 results in a decrease of the relative density (Figure 7 (b)). The same trend is observed when increasing scanning speed from 300 to 700 mm/s (Figure 7 (c)). Hence, the target relative density was only accomplished for the set of SLM parameters given in Table 2.

Table 2 - Optimized SLM parameters after density tests.

t [mm]	P [W]	h [mm]	v [mm/s]	$E_{density}$ [J/mm^3]
0,03	100	0,08	300	139

The density data is in good agreement with the observations made by optical microscopy, where it can be clearly seen that samples with lower relative density contain higher porosity levels (see Figure 6). The lower densities are therefore caused by the introduction of large pores, some of which are far from being spheriodized which would otherwise be less deleterious to the mechanical properties.

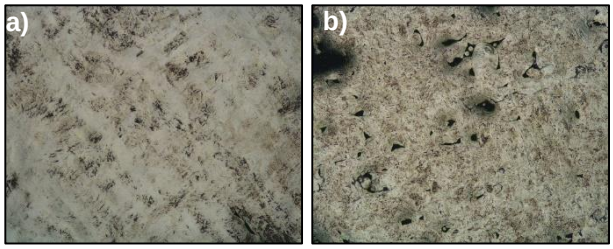

Figure 6 - Micrographs of SLM density specimens from batch 2: (a) top view of specimen 1 series 1 (99.09%), (b) top view of specimen 12 series 1 (97.49%).

Microstructural study

The top and side views of as-build (non-heat treated) Ti6Al4V samples produced by SLM are in Figure 8 a) and b). The top view indicates that a fully acicular α' martensitic microstructure was developed during the

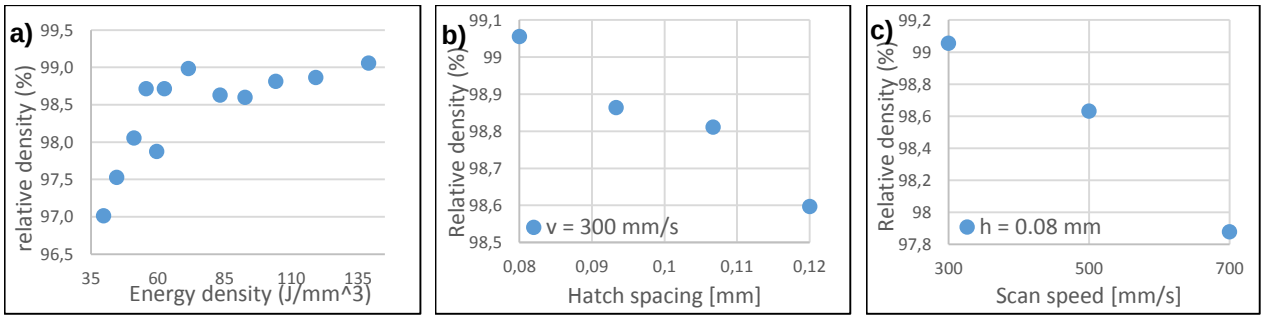

Figure 7 - Influence of a) energy density, b) hatch space and c) scan speed on the relative density in the batch 2 results.

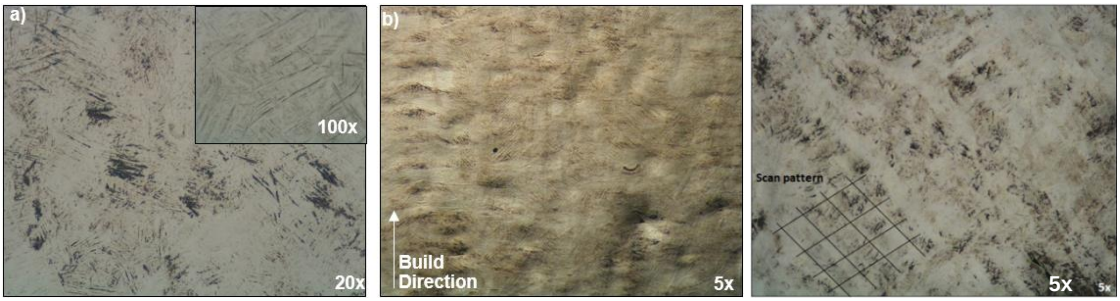

Figure 8 - (a) Top, (b) side view and (c) chessboard pattern in the top view of our untreated Ti6Al4V produced by SLM.

SLM process, as also noted by other authors on the bibliographical review (Subsection 2.5). The presence of the β phase is not observed.

During this work the scanning strategy used was the alternating zigzag (see Figure 3). This can be verified by observing the chessboard pattern on the top view as shown in Figure 8 c). The figure shows how the laser traced the lines slantwise, covering the surface diagonally. The effect of rotating the orientation 90º from layer to layer can also be noticed.

To improve the ductility of Ti6Al4V processed by SLM and to achieve desired mechanical properties, suitable heat treatments of the SLM samples must be carried out.

The attained microstructure after the heat treatment is shown in Figure 10. After heat treatment the fine martensitic structure has been transformed to a mixture of α and β. At 900 ºC, the β-fraction at high temperature is larger, reducing α-fraction comparing with lower temperatures [6]. In the micrograph the lighter phase is the α phase and the darks zones are the β phase, checked with the literature review [6].

Comparing Figure 8 and Figure 10 it can be said that the aim to get a coarser microstructure has been achieved.

Hardness

The Vickers hardness values for as-build and heat-treated Ti6Al4V samples are shown in Figure 9. These values show that the non-heat treated material is harder than the treated one, as it was expected due to the fact that α' martensitic microstructure is harder than the laminar α+ β microstructure. Furthermore it can be clearly seen that in the case of heat-treated samples the dispersion of HV values is much smaller, with all the values around 340 ± 20 HV, than those obtained from untreated samples ranging from 360 to 430 HV (395 ± 35 HV). This large dispersion is due to the difference of the behaviour that the as-built samples have near and far from their edges. The graph clearly shows that the hardness increases with the distance to the edge, reaching the highest values at the centre of the sample. In the graph the abscissa axis represents the position of each measurement, with 0% and 100% in the contours and 50% in the middle of the sample.

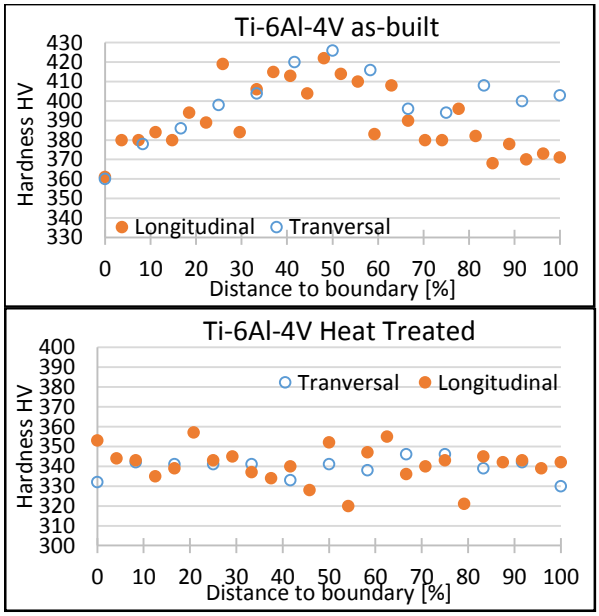

Figure 9 – Results of hardness analysis for as-built and heat treated samples.

Hardness values of bulk material from literature vary from 340 to 395 HV depending on thermal treatment. The hardness of SLM samples is higher, because during the process the melt poll cools down very rapidly when the laser beam has passed [15]. Hence, fast cooling gives rise to a martensitic α' phase. When heated, α

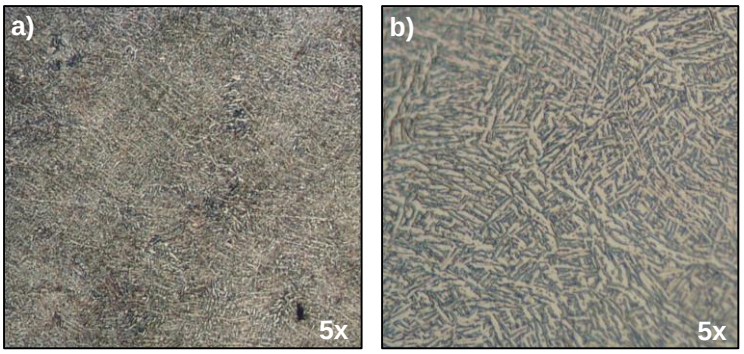

Figure 10 - Top view after heat treating at 900°C for 2h with furnace cooling. Lighter zones are α phase and the dark zones are the β phase.

Table 3 – Average results of the four combinations studied for tension test.

Combination	UTS [MPa]	σ_y [MPa]	Strain [%]	E [GPa]
As-built LD	831.5 ± 186.9	831.5 ± 186.9	0.87 ± 0.23	97.5 ± 20.6
As-built TD	749.2 ± 329.4	749.2 ± 329.4	0.89 ± 0.26	84.9 ± 11.3
Heat Treated LD	903.6 ± 153.8	885.9 ± 136.2	1.36 ± 1.89	112.5 ± 3.7
Heat Treated TD	830.4 ± 179.8	808.5 ± 157.8	1.32 ± 0.76	84.9 ± 22.4

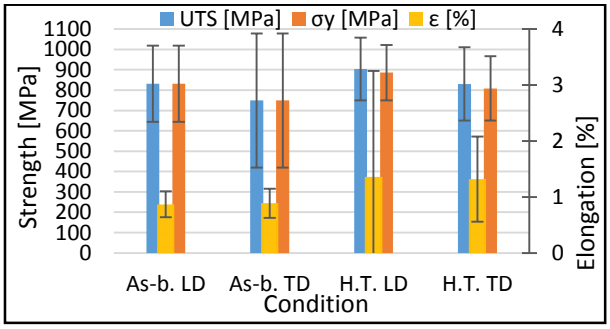

Figure 11 - Tension properties of as-fabricated and heat treated samples with different orientations.

phase is nucleated along the α' grain boundaries leading to the lamellar α+ β structure shown in Figure 10 b).

Tensile tests

From tensile strength results two main features are observed: the low ductility obtained even after heat treatment and the wide scatter of the results. Table 3 lists the average tensile strength data obtained for the four combinations studied: as-fabricated LD, as-fabricated TD, heat treated LD and heat treated TD. Figure 11 shows the tension properties of the four groups.

The fact that both the Young's modulus, the tensile strength and the yield strength are higher for the samples LD than their TD counterparts shows that there is a difference in the mechanical behaviour between the two orientations due to the anisotropy generated by the manufacturing process. The porosity defects are mainly between the layers with an oval shape (elongated in the direction perpendicular to the build direction). The LD parts, due to the geometry and orientation of the defects, when are tested tend to reduce the size of the defect due that the cross section is reduced, compacting layers with other layers. While the TD specimens tend to further open the defects, this being the reason why this orientation is critical.

Regarding to the heat treatment, the four properties are higher in the treated specimens than in the as-build ones. It is striking that the yield strength and the maximum tensile strength also follow the same trend. This it is not in line with the literature data (see ref. [6] and [7]), since it is observed that the normal trend is just the opposite, corroborating the hypothesis that premature failure of the specimens has occurred.

After the tensile tests the relative density of the specimens tested was measured to check the porosity of each one and whether this could be an important factor in the results or not. In all specimens a porosity below 0.8% was found.

Toughness

The Charpy test results at room temperature are shown in the Figure 12, where LD and TD refers to the building direction, parallel and perpendicular respectively.

The Charpy test results show that the LD specimens (5.98 ± 1.98 J) have absorbed less energy than TD ones 87.9 ± 1.3 J). The reason for the lower

toughness compared to literature (10.1 ± 0.5 J in ref. [2]), can be due to the presence of defects such as pores since porosity might cause a significant drop in toughness [19]. Other methods of measuring relative density ought to be used since Arquimedes´ method is likely to overestimate the relative density particularly in the case the pores still contain unmolten particles.

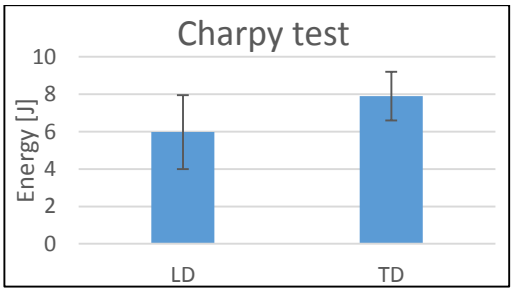

Figure 12 – The charpy test results for heat treated specimens.

Fractographic Analysis

In the Figure 13 images of the fracture of two specimens are shown, both of them heat treated but manufactured with different orientations (LD and TD).

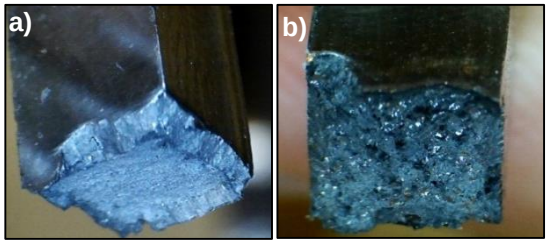

Figure 13 – USB Microscope images of heat treated specimens a) LD and b) TD.

Apparently, less defects in the LD samples might explain the differences in tensile strengths observed between LD and TD specimens.

In the SEM It is possible to observe the presence of pores with powder particles inside and particles that were not completely melted (see Figure 14).

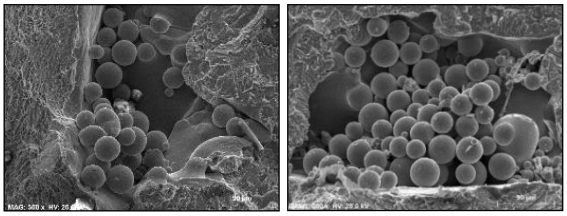

Figure 14 – SEM micrographs illustrating the present of defects.

According to Li et al. [20] balling phenomenon can be divided into two types: the ellipsoidal balls with diameters of around 500 µm and the spherical balls with dimensions of about 10 µm. The former is dependent on the wetting ability of the melt formed; the latter has no obvious detrimental effect to SLM quality. This phenomenon can be minimized by decreasing the oxygen content in the atmosphere to 0.1%. When severe balling phenomenon occurs, the metal balls may hinder the movement of the paving roller thereby preventing an homogenous powder particle distribution.

The morphology of the fracture surfaces, of the four combinations is shown in Figure 15. Again the difference between the heat treated, (c) and (d), and untreated samples, (a) and (b) is noted. The fracture surface of the as-build samples shows a brittle morphology where secondary cracking/unsealed pores are detected. Moreover in the fracture surface of the heat treated samples the secondary cracking is not observed and it presents a slightly more ductile morphology with micro dimples (Figure 15).

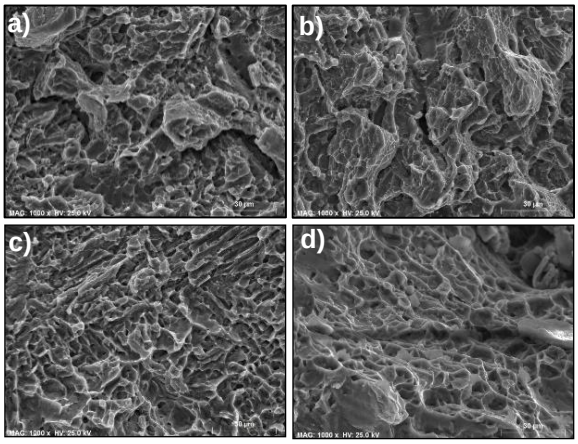

Figure 15 - Morphology of the fracture surface: a) 7_3, b) 2a_1, c) TT3 and d) TT7 specimens.

5. CONCLUSIONS

The main conclusions arising from the work developed are summarized as follows:

The parts produced by Selective Laser melting present a high roughness, non-comparable to that generated by traditional methods. Due to the high roughness, to the supports and to the surface where the supports are build the parts must be subjected to machining.

Due to the unique process conditions, such as temperature gradients and rapid cooling, heat treatment is required. Through the heat treatment carried out in this work (2 hours at 900 ° C followed by furnace cooling) a coarser microstructure, a reduction of the internal stresses and a decrease in hardness scatter along the surfaces were achieved.

Utilizing the optimal combination of the SLM and building parameters (the laser power, the scan velocity, the hatch space, the layer thickness, the energy density, the scan strategy, etc.) fully dense parts were obtained. In this work it was possible to achieve a relative density of around 99,6% compared to the Ti6Al4V density (4.43 g/cm3).

In hardness testing higher values compared to traditional processes were obtained. Hardness variation between outer areas and internal areas in the as-build samples was also observed. After heat treatment the hardness value is reduced as well as the boundary effect disappears.

The typical microstructure of the SLM process is the acicular α' martensitic phase in which the presence of the beta phase is not detected. This is observed in the as-build samples. After the heat treatment the fine martensitic structure becomes a mixture of α and β phase.

From the tensile test results it can be concluded that:

The SLM process generates anisotropy due to layer wise manufacturig.

The heat treated specimens achieve improved properties when compared to the as-build ones.

Under the conditions which were used (the powder characteristics, the selection of SLM parameters, the post processing treatments, the mechanical tests, etc.) a low ductility was obtained. After heat treatment there seems to be an apparent ductility increase which it is not possible to confirm due to the large scatter of the data.

In the tensile results two major problems are found. Firstly ductility values obtained are far from the expected ones and secondly, the scatter of the results for samples obtained under the same conditions is excessively high. Below some possible causes are listed:

- Porosity.

After the tensile tests the relative density of each sample was measured in order to verify the porosity was one of the possible causes, having high porosity involves large amount of defects. Acceptable relative density values were obtained in all the samples (all with lower porosity than 1%) and with no significant difference between each other. Therefore the porosity is not the only cause.

In SEM micrographs a large amount of defects, pores and partially melted particles are observed. Arquimedes´ method seems not to be the most suitable measurement technique to assess relative density.

- Contamination.

In SLM the material can be contaminated in three different ways before the manufacturing process, during the process or in the subsequent processes.

Regarding contamination before the manufacturing process basically focuses on the quality and characteristics of the powder used. Because of the importance played by the powder characteristics in the final quality of the parts, it is important to determine its parameters such as the composition, the average size and its particle size distribution, the geometry through the form factor and the phasic composition. In this dissertation this analysis was not performed.

The manufacturing by the SLM process was carried out under a tightly controlled inert argon atmosphere (purity 99.998%) to prevent contamination of the samples.

After the specimens were manufactured the only process where a contamination could occur was in the heat treatment. The heat treatment was performed under vacuum.

- Parameter selection.

Despite the high relative density measured, a large amount of defects and unmelted particles were observed in the SEM analysis of the fractured surfaces. Defects in the microstructure are a consequence of the parameterization of the machine.

In this work a high value of energy density (139 J/mm3), out the range recommended by the manufacturer 50 – 80 J/mm3, was used and higher relative density was obtained. This would explain the pools of melted region observed by SEM.

- Position in the build platform.

Another hypothesis is that the position of the samples on the production platform would affect the properties obtained because the inert gas flows from the right to the left side of the building chamber. The results were correlated with images of the build platforms and no direct relationship could be established.

- Machining operation

Both possible surface defects as asymmetries created in the specimens by the machining could lead to faulty results. This effect is discarded because the SEM micrograph clearly reveals that the internal defects are the main cause for the rupture.

In spite of not getting the expected results, work performed during this thesis is of great importance since it is the first time that this machine (SLM 125HL from CDRSP) has worked with titanium alloys. Therefore it can be said that it is the basis for further development studies towards refining of the SLM process of Ti6Al4V and gain experience and skills in operating the machine in order to be able to produce fully functional components.

References

[1] Antonysamy, A. A. (2012). Microstructure, texture and mechanical property evolution during additive manufacturing of Ti6Al4V alloy for aerospace applications. PhD Thesis, The University of Manchester, UK.

[2] Kruth, J. P., Badrossamay, M., Yasa, E., Deckers, J., Thijs, L., & Van Humbeeck, J. (2010). Part and material properties in selective laser melting of metals. In: Wan Sheng, Z., Jun, Y (Eds.). Proceedings of the 16th International Symposium on Electromachining, Shanghai Jiao Tong University Press, Shangai, China.

[3] Morgan, R., Sutcliffe, C. J., & O'neill, W. (2004). Density analysis of direct metal laser re-melted 316L stainless steel cubic primitives. Journal of Materials Science, 39(4), 1195-1205.

[4] Aliakbari, M. (2012). Additive Manufacturing: State-of-the-Art, Capabilities, and Sample Applications with Cost Analysis. Master of Science Thesis, Department of Industrial Production, KTH, June 2012.

[5] Kong, C. J., Tuck, C. J., Ashcroft, I. A., Wildman, R. D., & Hague, R. (2011, August). High density

Ti6Al4V via SLM processing: microstructure and mechanical properties. In Proc. of Solid Freeform Fabrication Symposium, Austin, Texas, USA, 2011, pp. 475-483.
[6] Vrancken, B., Thijs, L., Kruth, J. P., & Van Humbeeck, J. (2012). Heat treatment of Ti6Al4V produced by Selective Laser Melting: Microstructure and mechanical properties. Journal of Alloys and Compounds, 541, 177-185.
[7] Thomas Vilaro, Christophe Colin, and Jean-Dominique Bartout. As-fabricated and heat-treated microstructures of the ti-6al-4v alloy processed by selective laser melting. Metallurgical and Materials Transactions A, 42(10):3190-3199, 2011.
[8] Attar, E. (2011). Simulation of selective electron beam melting processes Ph. D. Thesis. University of Erlangen-Nuremberg.
[9] Agarwala, M., Bourell, D., Beaman, J., Marcus, H., & Barlow, J. (1995). Direct selective laser sintering of metals. Rapid Prototyping Journal, 1(1), 26-36.
[10] Kruth, J. P., Mercelis, P., Van Vaerenbergh, J., Froyen, L., & Rombouts, M. (2005). Binding mechanisms in selective laser sintering and selective laser melting. Rapid prototyping journal, 11(1), 26-36.
[11] S. Sun, Q. Liu, M. Bringezu, D. Shidid, M. Leary, B. Arhatari, M. Brandt. Microstructure and mechanical properties of Ti-6Al-4V parts built by selective laser melting. RMIT University, DSTO, La Trobe University, DMTC.
[12] Rombouts, M. (2006). Selective laser sintering/melting of iron-based powders PhD thesis, Katholieke Universiteit Leuven, Belgium.
[13] Campanelli, S. L., Contuzzi, N., Ludovico, A. D., Caiazzo, F., Cardaropoli, F., & Sergi, V. (2014). Manufacturing and Characterization of Ti6Al4V Lattice Components Manufactured by Selective Laser Melting. Materials, 7(6), 4803-4822.
[14] Cardaropoli, F., Alfieri, V., Caiazzo, F., & Sergi, V. (2012). Dimensional analysis for the definition of the influence of process parameters in selective laser melting of Ti-6Al-4V alloy. Proceedings of the Institution of Mechanical Engineers, Part B: Journal of Engineering Manufacture, 2012, 226, 1136–1142.
[15] Vandenbroucke, B., & Kruth, J. P. (2007). Selective laser melting of biocompatible metals for rapid manufacturing of medical parts. Rapid Prototyping Journal, 13(4), 196-203.
[16] Rehme, O. And Enmelmann, C., (2007), “Cellular Design for laser freeform fabrication Stuttgart: Proceedings of the fourth international WLT”- conference lasers in manufacturing 2007.
[17] Spierings, A. B., Schneider, M., & Eggenberger, R. (2011). Comparison of density measurement techniques for additive manufactured metallic parts.Rapid Prototyping Journal, 17(5), 380-386.
[18] Handbook, A. S. M. (2005). Volume 9. Metallography and Microstructures, 12.
[19] Yasa et al. Virtual and Physical Prototyping, vol 5, nº 2, 89 – 98, June 2010.
[20] Li, R., Liu, J., Shi, Y., Wang, L., & Jiang, W. (2012). Balling behavior of stainless steel and nickel powder during selective laser melting process. The International Journal of Advanced Manufacturing Technology, 59(9-12), 1025-10.